



DNA Nanocomposites Hot Paper

How to cite: *Angew. Chem. Int. Ed.* **2020**, 59, 19016–19020

International Edition: doi.org/10.1002/anie.202008471

German Edition: doi.org/10.1002/ange.202008471

Postsynthetic Functionalization of DNA-Nanocomposites with Proteins Yields Bioinstructive Matrices for Cell Culture Applications

Yong Hu, Carmen M. Domínguez, Sophina Christ, and Christof M. Niemeyer*

Abstract: We report on the directed postsynthetic functionalization of soft DNA nanocomposite materials with proteins. Using the example of the functionalization of silica nanoparticle-modified DNA polymer materials with agonists or antagonists of the epidermal growth factor receptor EGFR cell membrane receptor, we demonstrate that hierarchically structured interfaces to living cells can be established. Owing to the modular design principle, even complex DNA nanostructures can be integrated into the materials, thereby enabling the high-precision arrangement of ligands on the lower nanometer length scale. We believe that such complex biohybrid material systems can be used for new applications in biotechnology.

DNA-based hydrogels are on their way to becoming indispensable as a matrix for basic and applied biomedical research.^[1] These materials may have the same general properties as corresponding synthetic polymer-based hydrogels, such as high water content, biocompatibility and mechanical adaptability. However, they also possess the unique properties of nucleic acids, such as molecular recognition and programmability, biodegradability and, in particular, scalable architectures from nano- to micrometer scale.^[1b,2] Hence, by designing different DNA building blocks and optimizing their concentrations, the DNA hydrogels produced in this way can be tailored to desired applications, such as scaffolds for 3D cell culture and tissue engineering, controlled drug delivery systems and other uses in biomedicine.^[2a] With classical organic-chemical polymers, even more complex hydrogel systems can be built up by integrating nanomaterials into the polymer framework, resulting in mechanically reinforced and multifunctional biosubstrates.^[3] This has recently also been achieved with DNA hydrogels by synthesizing silica (SiNP)-DNA nanocomposite hydrogels whose components and mechanical

properties can be tailored to influence the behavior of eukaryotic cells.^[4] For a brief discussion of the differences between this novel composite material and more conventional polymers, see Figure S1 in the Supporting Information.

Despite these advances, the functionalization of DNA-based hydrogels with proteins is not yet well developed. Although examples of the non-specific embedding of proteins in DNA hydrogels have been described,^[5] there is a lack of systematic approaches to incorporate these highly specialized tools of nature into DNA polymers in a directed manner. While non-specific encapsulation approaches are well suited for the delivery and release of proteins, applications in the fields of cell culture and tissue engineering would require a stable and directional immobilization of proteins within the 3D matrix of a hydrogel. DNA-directed immobilization (DDI) of proteins is a powerful technique for the chemically mild and highly efficient directional binding of DNA-protein conjugates to produce micro- and nanostructured protein arrays on 2D surfaces.^[6] The use of the DDI method gives rise to 2D DNA materials that can often be applied in array format as a powerful tool for protein sensing and diagnostics.^[6,7] In recent years, such hard 2D DNA materials are also exploited used as functional surfaces for cell assays,^[8] for instance, to study signal cascades in living cells.^[9] In fact, by DDI of protein-decorated DNA origami nanostructures (DONs), even well-defined arrangements of protein ligands can be presented to adhered cells with full control over the ligand's number, stoichiometry, and precise nanoscale orientation.^[9] However, such a 2D arrangement of protein-DNA conjugates on planar substrates can hardly mimic the soft 3D extracellular matrix of natural tissues, for example to study complex cellular processes. On the other hand, the specifically directed functionalization of soft 3D materials with proteins has not yet been described.

To broaden the scope of functional nanostructured protein-DNA materials, we address here the issue of stable and directional protein immobilization within the 3D matrix of DNA hydrogels by using a postsynthetic hybridization-based method to modify soft DNA materials with protein functionality. Specifically, we engineered a recently developed SiNP-DNA nanocomposite material (shear modulus (G_0) of 3.2 Pa, as determined by multiple particle tracking microrheology)^[4] in such a way that binding loops are incorporated into the DNA backbone of the polymers during the synthesis of the materials by rolling circle amplification (RCA). These loops were then used for specific hybridization of protein-DNA conjugates or even protein-decorated DNA origami nanostructure (DON) constructs. We demonstrate the practicability of our approach by incorporating agonists and antagonists of the epidermal

[*] Dr. Y. Hu, Dr. C. M. Domínguez, M. Sc. S. Christ,
Prof. Dr. C. M. Niemeyer
Karlsruhe Institute of Technology (KIT), Institute for Biological
Interfaces (IBG 1)
Hermann-von-Helmholtz-Platz 1, 76344 Eggenstein-Leopoldshafen
(Germany)
E-mail: niemeyer@kit.edu

Supporting information and the ORCID identification number(s) for the author(s) of this article can be found under:
<https://doi.org/10.1002/anie.202008471>.

© 2020 The Authors. Published by Wiley-VCH GmbH. This is an open access article under the terms of the Creative Commons Attribution Non-Commercial NoDerivs License, which permits use and distribution in any medium, provided the original work is properly cited, the use is non-commercial, and no modifications or adaptations are made.

growth factor receptor (EGFR) into the soft composite materials to influence the activation of the EGFR in breast tumor cells.

To prepare the desired SiNP-DNA nanocomposite materials, DNA oligonucleotide-modified SiNPs were subjected to polymerization via RCA, similar as previously reported.^[4] However, the primer P and circular template oligomer T for RCA were modified to contain the 12-mer binding sequence 5'-(ATG)₄-3'. For a complete list of oligonucleotide sequences, see Table S1 in the Supporting Information. For the synthesis of the binding loop-modified SiNP-DNA nanocomposite material, in the following denoted as S^{BL} material, SiNPs (approx. 80 nm in diameter) were covalently conjugated with primer P, hybridized with template T, and the mixture was then subjected to RCA in the presence of dNTPs and Phi29 polymerase at 30 °C for 48 h. In the present study only thin films of the nanocomposite materials were prepared (thickness approx. 50 μm), in particular to meet the conditions of analysis by confocal laser scanning microscopy (CLSM). However, by upscaling the RCA reaction mixture, the dimensional scale of the present material films should be easily shiftable to the millimeter scale, as was shown with conventional DNA hydrogels.^[1a]

To verify that the so-produced materials indeed contain the engineered binding loops (L, Table S1), we initially investigated the hybridization with the complementary Cy3 fluorophore-labeled DNA oligonucleotide cL^{Cy3}, (5'-(CAT)₈-Cy3-3') (Figure 1). To this end, a commercial 4-well silicone gasket was mounted in a petri dish (see Figure S1) and individual wells were filled with S^{BL} material or, as a negative control, with a similar SiNP-DNA nanocomposite material bearing repetitive loops of the non-complementary scrambled sequence (S^{NC} material, in Figure 1). The materials were allowed to hybridize with cL^{Cy3} for 24 h at room temperature, washed repeatedly to remove unbound probe and analyzed by both wide-field (WF) microscopy and confocal laser scanning microscopy (CLSM). The results clearly showed that cL^{Cy3}

hybridized specifically with its complementary material resulting in a homogeneous labeling of the entire 3D matrix of the S^{BL} material (Figure 1b). Quantitative estimation of the binding efficiency indicated that about 35 binding loops per μm³ of the S^{BL} nanocomposites are accessible for hybridization with the complementary sequence cL (Table S2).

To further investigate the usefulness of our approach of postsynthetic modification, we wanted to make the materials suitable for cell culture experiments to study early stages of cell signalling by integrating specific protein functionalities. To this end, we selected agonists and antagonists of the epidermal growth factor receptor (EGFR). As an agonist, we chose the biotinylated epidermal growth factor (bEGF) polypeptide, to be functionalized with DNA oligomers via a covalent DNA-streptavidin (STV) conjugate.^[10] As an antagonist, we chose the monoclonal IgG antibody vectibix (VEC), which is well characterized as a strong inhibitor of the EGFR.^[11] The covalent protein-DNA conjugates containing STV or VEC, respectively, were synthesized from the 5'-thiol- and 3'-Cy3-labeled DNA oligonucleotide cL by using the heterobifunctional crosslinker sulfosuccinimidyl-4-(N-maleimidomethyl) cyclohexane-1-carboxylate (sSMCC), as previously described.^[12] The obtained conjugates, STV-cL^{Cy3} and VEC-cL^{Cy3}, were purified by fast protein liquid chromatography (FPLC) and characterized by gel electrophoresis (Figures S2-S4). The DNA-STV conjugate was coupled with bEGF to obtain the functional EGFR agonist.^[10]

The initial investigation of the specific binding of the so-prepared DNA-protein conjugates to S^{BL} materials was performed by a hybridization experiment, similar as described above. It is shown in Figure 2 that both EGF-STV-cL^{Cy3} and VEC-cL^{Cy3} hybridized specifically with S^{BL} materials bearing the complementary binding loops, whereas binding to the negative control materials occurred to a much lesser extent. Notably, CLSM images also showed that the entire 3D matrix of the S^{BL} material was homogeneously modified with the protein-DNA conjugates (lower two panels in Figure 2).

We then wanted to test whether substantially larger protein constructs can as well be used for postsynthetic

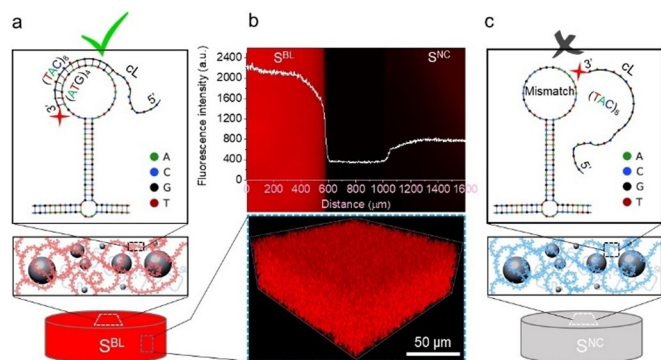


Figure 1. Postsynthetic modification of nanocomposite materials by hybridization with the Cy3-labeled DNA oligonucleotide cL. The schematics illustrate the experiments conducted with S^{BL} (a) and S^{NC} materials (c), mounted in two adjacent wells of a 4-well petri dish separated by a silicone barrier (500 μm +/−100 μm thickness, see also Figure S1). Wide-field fluorescence microscopy images (b) indicate that successful binding of cL only occurs with the S^{BL} material, whereas the negative control material (S^{NC}) shows only a weak increase in fluorescence. The 3D image in (b) was obtained by CLSM.

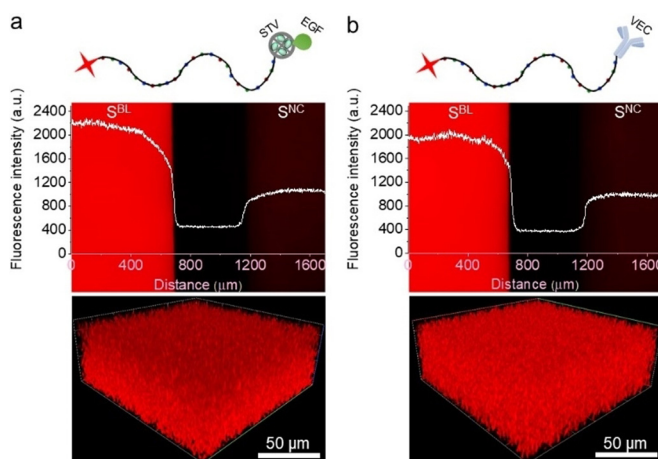


Figure 2. Functionalization of nanocomposite materials with protein-DNA conjugates EGF-STV-cL^{Cy3} (a) and VEC-cL^{Cy3} (b). 2D and 3D images were obtained by WF microscopy and CLSM, respectively.

modification of the S^{BL} materials. To this end, we chose a DNA origami nanostructure (DON), containing five STV moieties bound to the DON via biotin residues installed on one side of the rectangular DON plane (approx. $70 \times 100 \text{ nm}^2$).^[9] Furthermore, the DON was equipped with nine single-stranded oligonucleotides ($5'-(\text{CAT})_8-3'$) protruding from the opposite plane of the origami (Figure 3a, see also Figure S5) to enable specific hybridization with the loop sequence in the S^{BL} material. To enable visualization in fluorescence microscopy studies, the DON was also equipped with fluorescent labels, attached via Cy3-labeled staple strands. The characterization of the DON by atomic force microscope (AFM) confirmed the expected geometric arrangement of the STV proteins with an average occupancy of the contained biotin groups of 80% (Figure S6).

The STV-DON construct was further functionalized by incubation with bEGF (molar ratio of STV to bEGF = 1:1.8) for 1 h at room temperature (Figure 3a) and the mixture was then allowed to hybridize with S^{BL} and S^{NC} materials for 24 h at room temperature, as described above. After washing, the materials were analyzed by both WF microscopy and CLSM (Figure 3b). Despite the large size of the EGF-STV-DON^{Cy3} construct, specific hybridization occurred with a similar efficiency as observed for the smaller oligonucleotide and protein-DNA compounds. In fact, quantitative determination of the binding efficiencies revealed that EGF-STV-cL^{Cy3}, VEC-cL^{Cy3} and EGF-STV-DON^{Cy3} were bound in amounts of 10, 12, or 3 molecules per μm^3 of the S^{BL} nanocomposites, respectively (Table S2). Based on these numbers, the local concentration of agonist and antagonist moieties should be approximately equal for three different postsynthetically modified S^{BL} materials. We also verified the steric accessibility of the EGF and VEC moieties by immunostaining using specific antibodies directed against the proteins (Figure S7).

As the hydrogel materials displayed good biocompatibility (Figure S8),^[4] we then investigated whether the postsynthetically incorporated EGF and VEC moieties inside the hydrogel's matrix can be applied to trigger or suppress

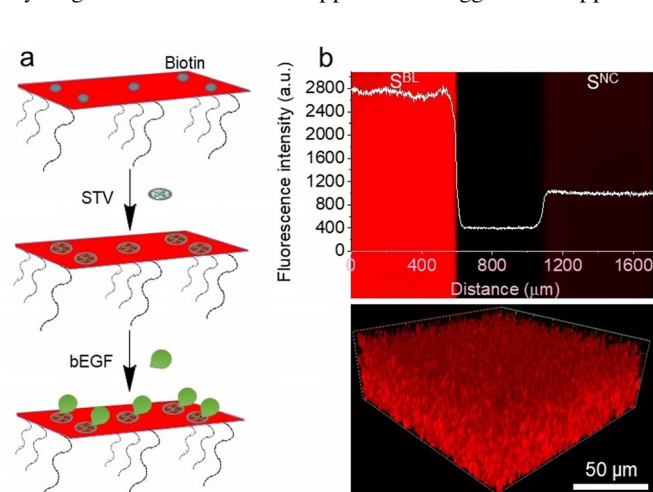


Figure 3. Functionalization of nanocomposite materials with protein-decorated DON. (a) Schematic drawing of the stepwise assembly of the EGF-STV-DON^{Cy3} construct. (b) Fluorescence WF images of S^{BL} materials modified with the EGF-STV-DON^{Cy3} construct. The 3D image underneath was obtained by CLSM.

activation of the EGFR in living cells (Figure 4). To this end, MCF7 cells stably expressing the EGFR genetically fused to enhanced green fluorescent protein (eGFP-EGFR) were seeded on the various hydrogels. Similar as observed before with unmodified S materials,^[4] these MCF7_{eGFP} cells migrated into the soft hydrogel matrix within 2 h (Figure S9). The cell-loaded materials were fixed and stained with DAPI to visualize the cell's nuclei as well as with a specific antibody recognizing the phosphorylated tyrosine 1068 residue of activated EGFR.^[10]

CLSM analysis revealed that MCF7_{eGFP} cells grown in S^{BL} materials postsynthetically functionalized with oligonucleotide cL showed a similar morphology as those grown in ligand-functionalized S^{BL} materials (Figure 4). Cells grown in VEC-modified S^{BL} material showed a high accumulation of the EGFR (green channel, in Figure 4) at the cell surface, suggesting that the VEC antibody tightly binds the receptor at the cell-materials interface (Figure 4b). Likewise, a high degree of EGFR accumulation was observed in the case of the EGF-modified materials (Figure 4c,d). This indicated that interaction between the EGFR and the EGF-ligands leads to the recruitment of the EGFR at the cell-material interface, similar as observed for planar solid substrates.^[10] Indeed, these hypotheses were supported by the distribution of the activated receptor (cyan channel). It is clearly evident that the amount of activated receptor was significantly lower in VEC-modified S^{BL} than in cL- and EGF-modified materials. Furthermore, in strong contrast, cells grown in the EGF-modified materials showed very high signals in the cyan channel (Figure 4c,d), indicating that the EGFR was switched on by the material-bound EGF moieties.

To further investigate the postsynthetic functionalization of DNA nanocomposite materials for cell study, we chose a carbon nanotube (CNT)-reinforced SiNP-DNA material (mass ratio of SiNP:CNT = 25:1, $G_0 = 8.5 \text{ Pa}$), which has increased entanglement and mechanical stiffness as compared

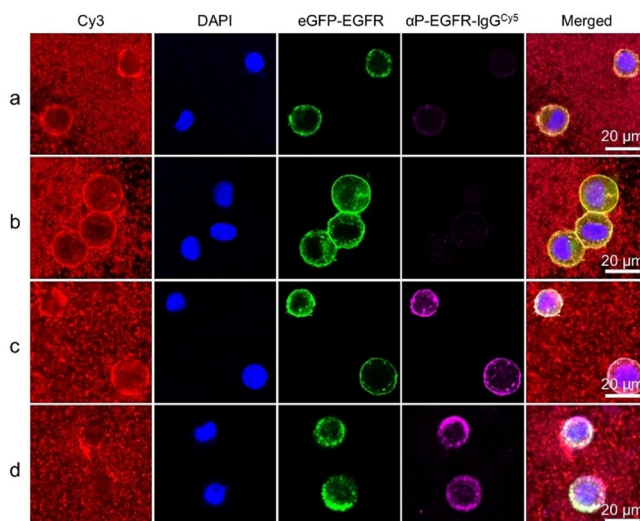


Figure 4. CLSM analysis of EGFR phosphorylation of MCF7_{eGFP} cells grown in the (a) cL^{Cy3}, (b) VEC-cL^{Cy3}, (c) EGF-STV-cL^{Cy3}, or (d) EGF-STV-DON^{Cy3} modified S^{BL} materials, respectively. For representative 3D images, see Figure S9.

to the S^{BL} materials (Figure S10). This SiNP/CNT-DNA (SC^{BL}) composite material was synthesized through copolymerization of primer-modified SiNPs and CNTs via RCA, similar as previously reported.^[4] The SC^{BL} composite materials were postsynthetically modified with cL^{Cy3} , $VEC-cL^{Cy3}$, $EGF-STV-cL^{Cy3}$ and $EGF-STV-DON^{Cy3}$ moieties, similar as described above for the S^{BL} materials. MCF7_{eGFP} cells grown in the functionalized SC^{BL} materials displayed similar effects of recruitment and activation of the EGFR at the cell-material interface (Figure S10), as observed for the correspondingly functionalized S^{BL} materials (Figure 4). Therefore, all observations consistently indicated that the postsynthetic decoration of DNA nanocomposite materials with proteins led to material systems that are stable under cell culture conditions and can be used to present ligands to transmembrane receptors of live cells. Although the investigations shown here focus on early stages of cell signaling, previous studies on the long-term cultivation (> 3d) of various cells, ranging from MCF7 over fibroblasts and embryogenic stem cells^[4] to bacteria^[13] indicate high stability of the S and SC materials, thus suggesting that late phases of cellular signaling cascades, such as induced gene expression, can also be investigated with these material systems.

Interestingly, we observed a considerable difference between EGF-STV- cL^{Cy3} and EGF-STV- DON^{Cy3} functionalized composite materials with respect to the phenotypic appearance of the MCF7_{eGFP} cells. All materials functionalized with cL^{Cy3} , $VEC-cL^{Cy3}$, or EGF-STV- cL^{Cy3} accumulated to a significant extent on the cell membrane (visible as red halos in the Cy3 channel in Figures 4, S10), whereas the EGF-STV- DON^{Cy3} functionalized materials were hardly enriched at the cell membrane (see also Figures S11 and S12). We hypothesize that this effect is due to the different spatial presentation of the EGF ligands. In the EGF-STV- cL^{Cy3} system, individual ligands are attached to the flexible backbone of the polymer. Since the activation of EGFR usually leads to the downstream internalization of the receptor,^[14] this process could further enhance the already preferred cellular uptake of SiNP-DNA materials.^[15] In contrast, the ligands of the EGF-STV- DON^{Cy3} system are presented on the relatively large and rigid surface of the DNA origami, which allows the activation of the receptors without their internalization, similar as previously demonstrated on planar glass substrates.^[9]

In conclusion, we here demonstrated for the first time the postsynthetic hybridization-based functionalization of soft DNA nanocomposite materials with proteins. The assembly of such protein-modified, hierarchically structured nanocomposites enables the targeted development of interfaces to living cells, as has been demonstrated here by using materials functionalized with agonists or antagonists of EGFR. Of particular importance is the high modularity of the design principle, which allows both the high-precision arrangement of ligands on the lower nanometer length scale and the targeted adjustment of the mesoscale mechanical and viscoelastic properties of the matrices. We therefore believe that our approach can be combined with refined methods of DNA polymer synthesis, protein-DNA conjugation chemistry and

microfluidic techniques to exploit such complex biohybrid material systems for new applications in biotechnology.

Acknowledgements

We acknowledge funding from the Helmholtz programme “BioInterfaces in Technology and Medicine” and Deutsche Forschungsgemeinschaft (GRK 2039). Y.H. is grateful to the China Scholarship Council (CSC) for his Ph.D. fellowship. This work was supported by the Alexander von Humboldt Foundation (Research Fellowship for C.M.D.). Open access funding enabled and organized by Projekt DEAL.

Conflict of interest

The authors declare that a patent application for SiNP-DNA composite materials has been filed.

Keywords: DNA nanocomposites · DNA origami nanostructure · epidermal growth factor receptor · phosphorylation · protein–DNA conjugates

- [1] a) D. Yang, M. R. Hartman, T. L. Derrien, S. Hamada, D. An, K. G. Yancey, R. Cheng, M. Ma, D. Luo, *Acc. Chem. Res.* **2014**, *47*, 1902–1911; b) J. Li, L. Mo, C.-H. Lu, T. Fu, H.-H. Yang, W. Tan, *Chem. Soc. Rev.* **2016**, *45*, 1410–1431; c) D. Wang, Y. Hu, P. Liu, D. Luo, *Acc. Chem. Res.* **2017**, *50*, 733–739; d) Y. Shao, H. Jia, T. Cao, D. Liu, *Acc. Chem. Res.* **2017**, *50*, 659–668; e) J. Gačanin, C. V. Synatschke, T. Weil, *Adv. Funct. Mater.* **2020**, *30*, 1906253.
- [2] a) Y. Zhang, J. Tu, D. Wang, H. Zhu, S. K. Maity, X. Qu, B. Bogaert, H. Pei, H. Zhang, *Adv. Mater.* **2018**, *30*, 1703658; b) Y. Hu, C. M. Niemeyer, *Adv. Mater.* **2019**, *31*, 1806294.
- [3] S. Merino, C. Martin, K. Kostarelos, M. Prato, E. Vazquez, *ACS Nano* **2015**, *9*, 4686–4697.
- [4] Y. Hu, C. M. Domínguez, J. Bauer, S. Weigel, A. Schipperges, C. Oelschlaeger, N. Willenbacher, S. Keppler, M. Bastmeyer, S. Heißler, C. Wöll, T. Scharnweber, K. S. Rabe, C. M. Niemeyer, *Nat. Commun.* **2019**, *10*, 5522.
- [5] a) L. Wan, Q. Chen, J. Liu, X. Yang, J. Huang, L. Li, X. Guo, J. Zhang, K. Wang, *Biomacromolecules* **2016**, *17*, 1543–1550; b) Xiang, K. He, R. Zhu, Z. Liu, S. Zeng, Y. Huang, Z. Nie, S. Yao, *ACS Appl. Mater. Interfaces* **2016**, *8*, 22801–22807; c) E. Kim, L. Zwi-Dantsis, N. Reznikov, C. S. Hansel, S. Agarwal, M. M. Stevens, *Adv. Mater.* **2017**, *29*, 1701086; d) E. Kim, S. Agarwal, N. Kim, F. S. Hage, V. Leonardo, A. Gelmi, M. M. Stevens, *ACS Nano* **2019**, *13*, 2888–2900.
- [6] R. Meyer, S. Giselbrecht, B. E. Rapp, M. Hirtz, C. M. Niemeyer, *Curr. Opin. Chem. Biol.* **2014**, *18*, 8–15.
- [7] a) C. M. Niemeyer, T. Sano, C. L. Smith, C. R. Cantor, *Nucleic Acids Res.* **1994**, *22*, 5530–5539; b) R. Wacker, H. Schroeder, C. M. Niemeyer, *Anal. Biochem.* **2004**, *330*, 281–287; c) R. C. Bailey, G. A. Kwong, C. G. Radu, O. N. Witte, J. R. Heath, *J. Am. Chem. Soc.* **2007**, *129*, 1959–1967; d) T. N. Tran, J. Cui, M. R. Hartman, S. Peng, H. Funabashi, F. Duan, D. Yang, J. C. March, J. T. Lis, H. Cui, D. Luo, *J. Am. Chem. Soc.* **2013**, *135*, 14008–14011; e) H. Xu, M. Gao, X. Tang, W. Zhang, D. Luo, M. Chen, *Small Methods* **2020**, *4*, 1900506.
- [8] A.-K. Schneider, C. M. Niemeyer, *Angew. Chem. Int. Ed.* **2018**, *57*, 16959–16967; *Angew. Chem.* **2018**, *130*, 17204–17212.

- [9] A. Angelin, S. Weigel, R. Garrecht, R. Meyer, J. Bauer, R. K. Kumar, M. Hirtz, C. M. Niemeyer, *Angew. Chem. Int. Ed.* **2015**, *54*, 15813–15817; *Angew. Chem.* **2015**, *127*, 16039–16043.
- [10] G. Arrabito, S. Reisewitz, L. Dehmelt, P. I. Bastiaens, B. Pignataro, H. Schroeder, C. M. Niemeyer, *Small* **2013**, *9*, 4243–4249.
- [11] J. M. Reichert, V. E. Valge-Archer, *Nat. Rev. Drug Discovery* **2007**, *6*, 349.
- [12] R. Wacker, C. M. Niemeyer, *Curr. Protoc. Nucleic Acid Chem.* **2005**, *Chapter 12*, Unit 12 17.
- [13] Y. Hu, D. Rehnlund, E. Klein, J. Gescher, C. M. Niemeyer, *ACS Appl. Mater. Interfaces* **2020**, *12*, 14806–14813.
- [14] A. Citri, Y. Yarden, *Nat. Rev. Mol. Cell Biol.* **2006**, *7*, 505–516.
- [15] A. Leidner, S. Weigel, J. Bauer, J. Reiber, A. Angelin, M. Grösche, T. Scharnweber, C. M. Niemeyer, *Adv. Funct. Mater.* **2018**, *28*, 1707572.

Manuscript received: June 15, 2020
Revised manuscript received: July 13, 2020
Accepted manuscript online: July 18, 2020
Version of record online: August 26, 2020